INELASTIC ANALYSIS OF STEEL FRAMES ACCOUNTING FOR STIFFNESS DEGRADATIONS

Lei Xu[1,*] and Yuxin Liu[2]

[1]*Canadian Cold Formed Steel Research Group*
Department of Civil Engineering, University of Waterloo
Waterloo, Ontario, Canada N2L 3G1
**(Corresponding author: E-mail: lxu@uwaterloo.ca)*
[2]*Atomic Energy of Canadian Limited (AECL)*

Received: 13 July 2005; Revised: 5 May 2006; Accepted: 6 May 2006

ABSTRACT: This paper presents a method for nonlinear inelastic analysis of steel frameworks considering both flexural and shearing stiffness degradations in the inelastic range. With the introduction of the so-called stiffness degradation factors to characterize stiffness deterioration associated with inelastic flexural and shearing deformations, the stiffness matrix for a beam-column member is formed as in the conventional matrix displacement method of analysis. In deriving the stiffness coefficients, geometrical nonlinearity and shear deformation (Timoshenko beam model) are taken into consideration. The material constitutive models account for nonlinear behaviour under single and/or combined stress states. The computational model allows the incremental procedure to reach loading levels at which instability and/or plastic mechanisms occur. Also accounted for in the computational model is the influence of residual stresses on initial-yield and full-yield capacities of members. The proposed nonlinear analysis method is applied for three steel frame examples. Comparisons between the proposed method and other published methods are presented. The results suggest that the proposed method realistically accounts for geometrical nonlinearity and inelastic flexural and shearing behaviour, and is computationally efficient.

Keywords: Nonlinear analysis, inelastic behavior, stiffness degradation, shear deformation, steel frameworks

1. INTRODUCTION

To capture the realistic behavior of steel frameworks under the action of different load conditions, nonlinear structural analysis has recently received more attention in the structural engineering community. The development of computer-based techniques in the last four decades, such as the matrix method and finite element method, allow engineers to extend linear elastic analysis to more realistic nonlinear analysis (McGuire et al. [1]). It is worth noting that geometrical nonlinearity accounting for P-Δ of frames and P-δ of members can result in accurate results as required using nonlinear analysis, assuming the materials to be in the elastic range. The results, however, may be inaccurate since the effect of material inelasticity is ignored. Although the influences of geometrical and material nonlinearities on structure responses must be considered in the design codes (CISC [2], AISC [3], CEN [4]), there is no clear stipulation that requires a designer to take a structure as a whole system and conduct nonlinear structural analysis and design. Instead, some of the nonlinear effects are partially accounted for in the design formulas by means such as P-δ amplification factors and effective length factors in component-based design of structures.

To facilitate the analysis and design of steel frames, many studies have been devoted to develop more practical methods of nonlinear analysis during the last decade. Methods such as the inelastic limit states design (Ziemian et al. [5]) and advanced analysis (Chen and Toma [6]) attempted to bring computer-based nonlinear analysis into the design of steel frames. Current second-order inelastic analysis methods for framed structures may be categorized as being either a "plastic-hinge" or a "spread-of-plasticity" approach. The former assumes that member plasticity is concentrated in zero-length regions (e.g., plastic hinges that form at the ends of the member). The section behavior changes abruptly from purely elastic to fully plastic once the corresponding moment reaches a level that satisfies the predefined yield criterion (Orbison et al. [7]). Because of

the simplicity, the plastic-hinge method has been applied to a large extent in the inelastic analysis of framed structures (e.g., Chen et al. [8]). However, as later research showed that the plastic-hinge method of second-order analysis could overestimate the member strength, the spread-of-plasticity approach was introduced to address this shortcoming (King et al. [9]). The spread-of-plasticity approach could be implemented from different techniques. For instance, the spread of plasticity in a member was modeled either by a tapered element attached to the member ends (Acroyd [10]), or by dividing the entire member as a collection of segments with variable *EI* over the member length (Cook [11]). Alternatively, plasticity could also be gradually traced by introducing higher-order displacement fields in the member stiffness formulation (Espion [12]). The fiber-element method proposed by Powell and Chen [13]) discretized a member both along its length and through its cross-section depth to trace the gradual spread of plasticity. Employing an integration technique to find flexibility coefficients that permitted the formation of the incremental member stiffness matrix accounting for the effect of the spread of plasticity, the quasi-plastic-hinge method provided a reasonable description of the gradual degradation of member stiffness (Attalla et al. [14]). Compared to the fiber-element method, the quasi-plastic-hinge method is computationally more efficient and accurate. More recently, a three-plastic-hinge model has been proposed to account for both geometrical nonlinearity and material inelasticity (Chan and Zhou [15]).

This study concerns planar steel frameworks discretized as an assembly of beam-column members that have compact sections for which plastic deformation is not precluded by local buckling (AISC [3]). A computer-based method for the nonlinear analysis of planar steel frameworks is presented. The method is based on Timoshenko beam theory [16] which explicitly accounts for the influence of shear deformation and geometrical nonlinearity on elastic behaviour of members (Timoshenko and Gere [16], Chugh [17]). In addition, the inelastic behavior of members under combined moment plus axial force and moment plus shear force are taken into consideration. Stability functions are employed to model the effect of axial force on the elastic flexural stiffness of members (Chen et al. [8], Chen and Lui [18]), and the influence of residual stresses on the initial-yield and full-yield capacities of members is taken into account. The proposed nonlinear inelastic analysis procedure is a direct extension of the conventional matrix displacement method of linear-elastic analysis. The stiffness degradation factors are applied to progressively deteriorate the inelastic flexural and shearing stiffness properties of framework members over an incremental load history. The proposed method is then verified with three steel structures from other researchers (Chen et al. [8], Attalla et al. [14], Kanchanalai [19], Driscoll and Beedle [20]).

2. INELASTIC MODEL OF BEAM-COLUMN MEMBER

Consider the prismatic planar beam-column member in Figure 1, where L = member length, E = material Young's modulus, G = material shear modulus, I = cross-section moment of inertia, A = cross-section area, and A_s = equivalent shear area. To account for the stiffness degradation, parameters R_j and T_j (j =1, 2) are the flexural and translational shearing tangent stiffnesses at both ends of a member. Parameters r_j and t_j (j =1, 2) are referred to as flexural and shear stiffness degradation factors, which are determined by the corresponding tangent stiffness. Notations f_i and d_i (i =1, 2, ..., 6) are used to express the local-axis member-end forces and deformations, respectively.

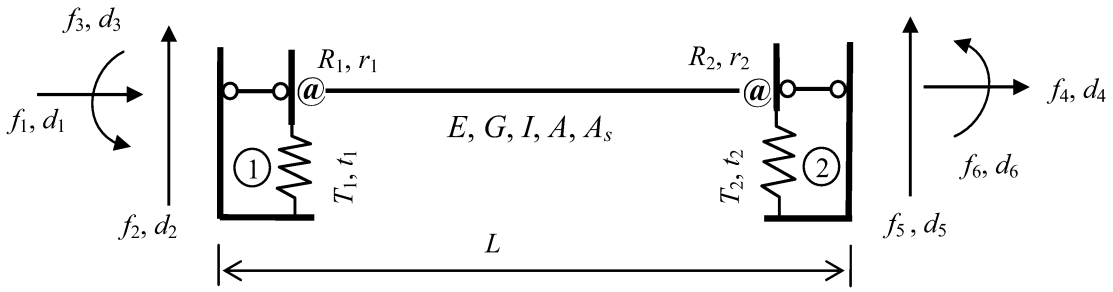

Figure 1. Beam-column Member Model

2.1 Inelastic Flexural Stiffness

The variation of inelastic flexural stiffness for a cross section of a beam-column member can be characterized by a moment-curvature (M–ϕ) curve as shown in Figure 2, where M_y is the moment capacity of the section at the initial-yield state; M_p is the corresponding full-yield moment capacity, accounting for primary and residual stresses (Huber and Beedle [21]); and ϕ_p, called the plastic limit curvature, can be interpreted as the plastic deformation beyond initial yielding at which the section fully yields. The quantity $dM/d\phi = R$ is the inelastic flexural stiffness of the section while r is the corresponding flexural stiffness degradation factor. With little error for most wide flange section shapes commonly used in steel framing construction (Hasan et al. [22], Liu [23]), the continuous nonlinear portion of the M–ϕ curve in Figure 2 can be modeled as an elliptical shape defined by the function,

$$\begin{aligned} &M = M_y + (M_p - M_y)[1-(1-\phi/\phi_p)^{e_0}]^{1/e_0}; \\ &0 \le \phi/\phi_p < 1; \quad M_y/M_p \le M/M_p \le 1 \end{aligned} \tag{1}$$

where the exponent $e_0 > 1$ is associated with the cross-section shape of the member and is to be determined by experimental tests. If $M \le M_y$, then the inelastic deformation $\phi = 0$, while if $M_y \le M \le M_p$, the inelastic deformation is, from Eq. (1),

$$\begin{aligned} &\phi = \phi_p - \phi_p\{1-[(M-M_y)/(M_p-M_y)]^{e_0}\}^{1/e_0}; \\ &0 \le \frac{\phi}{\phi_p} \le 1; \quad \frac{M_y}{M_p} \le \frac{M}{M_p} \le 1 \end{aligned} \tag{2}$$

Upon differentiating Eq. (1) with respect to inelastic curvature ϕ, the inelastic flexural stiffness is given by,

$$\begin{aligned} &R = \frac{dM}{d\phi} = \frac{(M_p - M_y)}{\phi_p}(1-\phi/\phi_p)^{e_0-1}[1-(1-\phi/\phi_p)^{e_0}]^{(1-e_0)e_0}; \\ &0 \le \frac{\phi}{\phi_p} \le 1; \quad \frac{M_y}{M_p} \le \frac{M}{M_p} \le 1 \end{aligned} \tag{3}$$

where $R = \infty$ if inelastic curvature $\phi = 0$, while $R = 0$ if $\phi \ge \phi_p$ as shown in Figure 2.

Similar to the definition of the end-fixity factor for semi-rigid members (Xu and Grierson [24]), the stiffness degradation factor, r, is defined by the ratio of elastic deformation to inelastic deformation at a member section and is given by,

$$r = 1/(1+3EI/RL) \tag{4}$$

which indicates that if r = 1, the section remains completely elastic ($R = \infty$), while if r = 0, the section is fully plastic (R = 0). A value of r between zero and one denotes that the section is in the inelastic state.

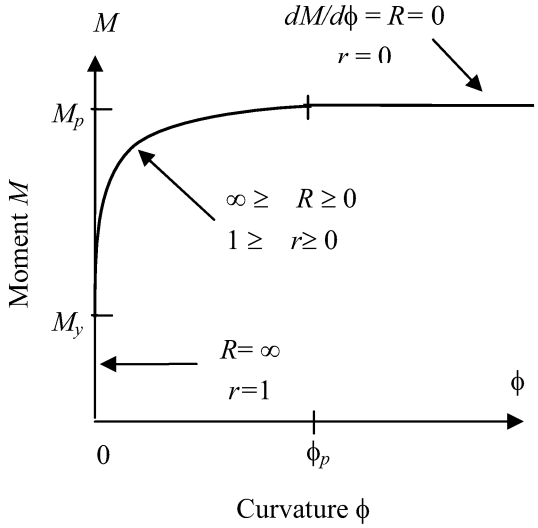

Figure 2. Post-elastic Moment-curvature Curve

2.2 Transverse Shear Stiffness

Transverse shear stiffness of a cross section, T, can be determined by the relationship between shear force V and transverse deflection δ on the basis of experimental results. To this end, the test results obtained by Hall and Newmark [25] are employed to determine the V-δ relationship and derive the corresponding transverse shear stiffness T. Hall and Newmark [25] proposed the following shear stress and strain expressions based on testing the wide flange steel section W8×58:

$$\gamma = \begin{cases} \tau/G & (0 \le \gamma < 0.00143 \text{ mm/mm}; 0 \le \tau < 113.685 \text{MPa}) \\ \dfrac{\tau - 110.653}{2115.23} & (0.00143 \le \gamma < 0.02; 113.685 \le \tau < 152.958 \text{MPa}) \\ (\tau/482.3)^{3.4} & (0.02 \le \gamma < 0.3; 152.958 \le \tau < 338.299 \text{MPa}) \end{cases} \tag{5}$$

where γ and τ are shear strain and shear stress, respectively. It can be seen from Eqs. (5) that the initial yield stress τ_y = 113.685 MPa corresponds to shear strain γ_y = 0.00143 mm/mm, and the limits of plastic stress and strain are approximate values τ_p = 338.299 MPa and γ_p = 0.3 mm/mm. Although Eqs. (5) were obtained from experimental data based on W8×58 section, the obtained γ-τ relationship was suggested for estimating the shear deflections of other mild-steel wide-flange sections (Hall and Newmark [25]).

Taking the effective shear area $A_s = t_w(d\text{-}t_f)$, where t_w = web thickness, d = beam depth, t_f = flange thickness, the shear force of the cross section can be expressed as $V = \tau A_s$. The transverse shear deflection can be evaluated by $\delta_s = \gamma l_s$, where l_s is a segmental length along the beam and is taken as the unit length to facilitate analysis. Hereinafter, the V-δ curve may be interpreted as the relationship between shear force and the deflection at a critical section, and the nondimensional expressions of Eqs. (5) can be readily given by,

$$\frac{\delta}{\delta_p}=\begin{cases}0.0142\dfrac{V}{V_p} & \left(0\le\dfrac{\delta}{\delta_p}<0.00477;0\le\dfrac{V}{V_p}<0.336\right)\\ 0.533\dfrac{V}{V_p}-0.174 & \left(0.00477\le\dfrac{\delta}{\delta_p}<0.067;0.336\le\dfrac{V}{V_p}<0.452\right)\\ \left(\dfrac{V}{V_p}\right)^{3.4} & \left(0.067\le\dfrac{\delta}{\delta_p}<1;0.452\le\dfrac{V}{V_p}<1\right)\end{cases} \quad (6)$$

in which V_p and δ_p are the plastic shear strength and plastic shear deformation, respectively. Equation (6) is shown in Figure 3(a) as the dashed curve based on the experimental results given in Eq. (5) obtained from Hall and Newmark [25]. It can be seen from Figure 3(a) that the elastic deflection is so small that it can be neglected, and the plastic shear strength is about three times that of the initial yield shear strength of the section.

To determine transverse-shear stiffness T for the purpose of inelastic analysis, employing curve-fitting technique, the normalized shear force-deflection relationship in the inelastic stage as in Eq. (6), can be expressed as,

$$\frac{\delta_i}{\delta_{ip}}=1-\left[1-\left(\frac{V-V_y}{V_p-V_y}\right)^{1.5}\right]^{1/1.5} \qquad \left\{0\le\frac{\delta_i}{\delta_{ip}}<1;\ \ \frac{V_y}{V_p}\le\frac{V}{V_p}<1\right\} \quad (7)$$

where δ is the inelastic shear deflection which excludes the initial yield shear deflection; δ_{ip} is the plastic shear deflection which excludes initial yield deflection; and V_y is the initial yield strength, respectively. Based on the experimental results shown in Figure 3(a) for the dashed curve (Hall and Newmark [25]), $\delta_{ip} = 0.3$ and $V_p = 3\ V_y$, Eq. (7) is plotted as the solid curve in Figure 3(a). It is clear from the figure that Eq. (7) is in good agreement with the experimental-fitting curve Eqs. (6b) and (6c). Therefore, Eq. (7), a transition curve from initial yield to fully plastic state, is employed in this study.

The inelastic behavior of shear force-deflection relationship for a frame member is graphically shown in Figure 3(b) based on Eq. (7). If the material at the neutral axis of a wide flange cross section experiences initial shear yielding, which is shown at point B in Figure 3(b), initial yield shear force V_y is reached. Then, with increasing shear force, plastic yielding spreads across the section depth as described in Eq. (7) until plastic shear strength V_p is reached at point C.

In the range between initial-yield and fully-plastic states, degraded shear stiffness T can be derived as follows. Based on Eq. (7), the transverse shear stiffness T of a cross section can be found as,

$$T=\frac{dV}{d\delta_i}=\frac{V_p-V_y}{\delta_{ip}}\sqrt{\frac{V_p-V_y}{V-V_y}}\sqrt[3]{1-\left(\frac{V_p-V_y}{V-V_y}\right)^{1.5}} \quad (8)$$

and having this inelastic stiffness T be determined, similar to the case of flexural bending, the shear stiffness degradation factor t at the critical section of a member is defined as,

$$t = 1/(1+3EI/TL^3) \tag{9}$$

It can be seen from Eqs. (8), (9) and Figure 3(b) that, before the applied shear force reaches V_y, the section remains elastic ($T = \infty$ or $t = 1$); whereas after $V = V_p$, the section is fully plastic, and shear stiffness degrades to zero ($T = 0$ or $t = 0$). A value of t between zero and one denotes that the cross section is in the inelastic state.

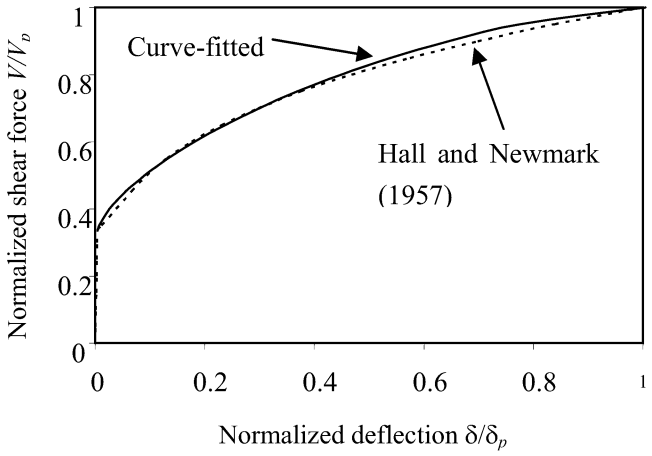

(a) Elastoplastic relationship

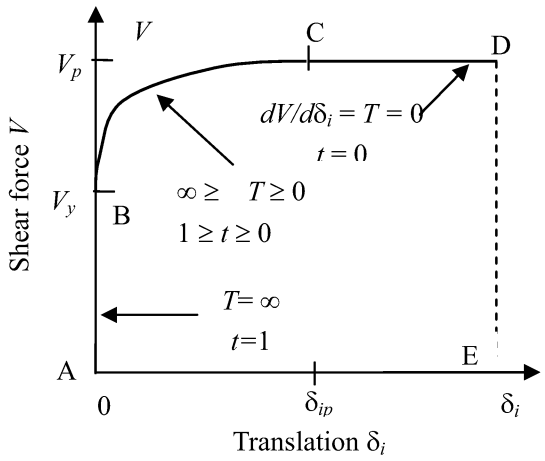

(b) Post-elastic relationship

Figure 3. Shear Force-deflection Curves

3. MEMBER STIFFNESS MATRIX

Having the inelastic stiffnesses R, T and the corresponding degradation factors r, t, the inelastic force-deformation relationship for the beam-column member shown in Figure 1 is given by

$$\boldsymbol{f} = \boldsymbol{kd} \tag{10}$$

where the vectors of end-section forces $f = [f_1, f_2, \ldots f_6]^T$ and deformations $d = [d_1, d_2, \ldots d_6]^T$ are referenced to the local-axis system for the member. The local-axis stiffness matrix for the member is,

$$\boldsymbol{k} = \begin{bmatrix} k_{11} & 0 & 0 & k_{14} & 0 & 0 \\ & k_{22} & k_{23} & 0 & k_{25} & k_{26} \\ & & k_{33} & 0 & k_{35} & k_{36} \\ & & & k_{44} & 0 & 0 \\ & Sym & & & k_{55} & k_{56} \\ & & & & & k_{66} \end{bmatrix} \tag{11}$$

The stiffness coefficients k_{ij} (i, =1, 2,…6; j =1, 2,…6) in Eq. (11) take into account the influences that both axial force and shear deformation have on elastic flexural stiffness (i.e., Timoshenko beam theory), as well as the degradation in flexural stiffness due to plastic deformation. In the derivation, the force method, displacement method, and moment distribution method were employed to find the coefficients for the element model shown in Figure 1 (Liu [23]). The related formulas are summarized as follows. The axial stiffness coefficients

$$k_{11} = k_{44} = -k_{14} = -k_{41} = EA/L \tag{12}$$

are the same as in conventional elastic analysis. The rest coefficients are given by

$$k_{22} = k_{22}^r \chi_1 = k_{55} = -k_{25} = -k_{52} \tag{13a}$$

$$k_{23} = k_{23}^r \chi_1 = k_{32} = -k_{35} = -k_{53} \tag{13b}$$

$$k_{26} = k_{26}^r \chi_1 = k_{62} = -k_{56} = -k_{65} \tag{13c}$$

$$k_{33} = k_{33}^r \chi_2 \tag{13d}$$

$$k_{36} = k_{36}^r \chi_3 = k_{63} \tag{13e}$$

$$k_{66} = k_{66}^r \chi_4 \tag{13f}$$

In the foregoing expressions, the stiffness coefficients

$$k_{22}^r = \frac{EI}{L^3\Omega}\left\{3b\eta_1(1+c\eta_2)[6r_1r_2 + b\eta_1(1-c\eta_2)(r_1+r_2-2r_1r_2)] + P\frac{L^2\Omega}{EI}\right\} \tag{14a}$$

$$k_{23}^{r}=\frac{3b\eta_1 EIr_1(1+c\eta_2)}{L^2\Omega}[b\eta_1(1-r_2)(1-c\eta_2)+3r_2] \tag{14b}$$

$$k_{26}^{r}=\frac{3b\eta_1 EIr_2(1+c\eta_2)}{L^2\Omega}[b\eta_2(1-r_1)(1-c\eta_2)+3r_1] \tag{14c}$$

$$k_{33}^{r}=3r_1 b\eta_1 EI[b\eta_1(1-r_2)(1-b^2\eta_2^2)+3r_2]/(L\Omega) \tag{14d}$$

$$k_{36}^{r}=9bc\eta_1\eta_2 EIr_1r_2/(L\Omega) \tag{14e}$$

$$k_{66}^{r}=3r_2 b\eta_1 EI[b\eta_1(1-r_1)(1-c^2\eta_2^2)+3r_1]/(L\Omega) \tag{14f}$$

account for flexural stiffness degradation in the inelastic state through factors r_1 and r_2, while the following factors:

$$\chi_1=\frac{t_1t_2}{t_1t_2+4\beta(t_1+t_2-2t_1t_2)} \tag{15a}$$

$$\chi_2=1-\frac{b\eta_1r_1}{4\Omega\beta}\frac{(1+c\eta_2)^2[b\eta_1(1-r_2)(1-c\eta_2)+3r_2]^2}{b\eta_1(1-r_2)(1-c^2\eta_2^2)+3r_2}(1-\chi_1) \tag{15b}$$

$$\chi_3=1-\frac{b\eta_1(1+c\eta_2)^2}{12c\eta_2\Omega\beta}[b\eta_1(1-r_1)(1-c\eta_2)+3r_1][b\eta_1(1-r_2)(1-c\eta_2)+3r_2](1-\chi_1) \tag{15c}$$

$$\chi_4=1-\frac{b\eta_1r_2}{4\Omega\beta}\frac{(1+c\eta_2)^2[b\eta_1(1-r_1)(1-c\eta_2)+3r_1]^2}{b\eta_1(1-r_1)(1-c^2\eta_2^2)+3r_1}(1-\chi_1) \tag{15d}$$

account for shear stiffness degradation in inelasticity through factors t_1 and t_2.

The parameter P in Eq. (14a) denotes axial force, while in Eqs. (14) and (15), the parameters

$$b=\begin{cases}\dfrac{1-\psi/\tan\psi}{\tan(\psi/2)/(\psi/2)-1} & P\le 0\\[2ex] \dfrac{1-\psi/\tanh\psi}{\tanh(\psi/2)/(\psi/2)-1} & P>0\end{cases} \tag{16a}$$

$$c=\begin{cases}\dfrac{\psi-\sin\psi}{\sin\psi-\psi\cos\psi} & P\le 0\\[2ex] \dfrac{\psi-\sinh\psi}{\sinh\psi-\psi\cosh\psi} & P>0\end{cases} \tag{16b}$$

in which,

$$\psi = \begin{cases} L\sqrt{\dfrac{-P/EI}{1+P/GA_s}} & P \le 0 \\ L\sqrt{\dfrac{P/EI}{1+P/GA_s}} & P > 0 \end{cases} \tag{16c}$$

are well-known stability functions that account for the influence of axial force on elastic flexural stiffness (Chen et al. [8]), and the factors

$$\eta_1 = (1+P/GA_s)(1+\xi f_1)/(1+\xi f_2) \tag{17a}$$

$$\eta_2 = (1+\xi f_3)/(1+\xi f_1) \tag{17b}$$

in which,

$$\xi = \frac{EI(1+P/GA_s)}{GA_sL^2} \tag{17c}$$

$$f_1 = \begin{cases} \psi^2/(1-\psi/\tan\psi) & P \le 0 \\ -\psi^2/(1-\psi/\tanh\psi) & P > 0 \end{cases} \tag{17d}$$

$$f_2 = \begin{cases} \psi^3\tan(\psi/2)/[\tan(\psi/2)-\psi/2] & P \le 0 \\ -\psi^3\tanh(\psi/2)/[\tanh(\psi/2)-\psi/2] & P > 0 \end{cases} \tag{17e}$$

$$f_3 = \begin{cases} \psi^2/(1-\psi/\sin\psi) & P \le 0 \\ -\psi^2/(1-\psi/\sinh\psi) & P > 0 \end{cases} \tag{17f}$$

account for the influence of shear deformation on elastic flexural stiffness.

Finally, in Eqs. (14)-(15) and (16)-(17), the parameter

$$\Omega = 9r_1r_2 + 3r_2b\eta_1(1-r_1) + 3r_1b\eta_1(1-r_2) + b^2\eta_1^2(1-r_1)(1-r_2)(1-c^2\eta_2^2) \tag{18}$$

while in Eqs. (15), the parameter

$$\beta = \frac{L^3}{12EI}k_{22}^r \tag{19}$$

4. COMBINED LOADING

For a steel framed structure, columns generally experience significant axial load plus moment, while beams may experience significant moment plus shearing force. The analysis model presented thus far has considered a planar beam-column member that experiences inelastic behavior due to bending or shearing alone. Therefore, the stiffness degradation associated with the combined loading cases needs to be addressed.

4.1 Moment Plus Axial Effect

The inelastic model of beam-column members is extended to combined bending moment plus axial force case. Under some combination of applied bending moment M and axial force P, initial yielding of a member section is governed by the normalized initial-yield criterion,

$$M / M_y + P / P_y = 1 \tag{20}$$

while full yielding of the section can be taken as being governed by the normalized full-yield criterion,

$$M / M_P + (P / P_p)^{\alpha} = 1 \tag{21}$$

where the moment and axial force initial-yield and full-yield capacities are M_y, P_y and M_p, P_p, respectively, and the exponent α in Eq. (21) depends on the shape of the member section, e.g., α = 1.3 for a wide-flange steel section (Duan and Chen [26]). The inelastic response domain for the member section is the shaded area in Figure 4 bounded by Eq. (20), plotted as the linear initial-yield line, and Eq. (21), plotted as the nonlinear full-yield line.

As shown in Figure 4, the region of influence in the inelastic response domain for a particular combination of moment M plus axial force P is defined by the angle of inclination θ of the straight line that passes through the origin point O_o and points O_y and O_p corresponding to the initial-yield and the full-yield of the section, respectively. It is noted that the assumption that the ratio M/P remains constant throughout the response domain is made solely to facilitate the assignment of stiffness degradation factors discussed in the following, and has no effect otherwise on the analysis. Figure 4 also indicates that the point O_y corresponds to reduced initial-yield moment and axial force capacities M_{yr} and P_{yr}, respectively, while the point O_p corresponds to reduced full-yield moment and axial force capacities M_{pr} and P_{pr}, respectively, where the subscript r stands for the reduced capacity. Having, from the analysis, the coordinates (M_{yr}/M_p, P_{yr}/P_p) of the initial-yield point O_y for a particular combination of M plus P causing plastic deformation at an end section of a beam-column member, the angle of inclination of line O_o-O_y-O_p in Figure 4 is readily found as,

$$\theta = \tan^{-1}[(P_{yr} M_p) / (M_{yr} P_p)] \tag{22}$$

which is employed to determine the loading path and the reduced initial and full capacities of axial forces and bending moments. Thus, having the reduced first-yield and full-yield moment capacities M_{yr}, and M_{pr} determined, the inelastic flexural stiffness R accounting for the combined bending moment and axial force case can be facilitated by replacing the moment capacities M_y and M_p in Eq. (3) with associated reduced moment capacities M_{yr} and M_{pr}, respectively. The corresponding flexural stiffness degradation factor r can then be computed from Eq. (4).

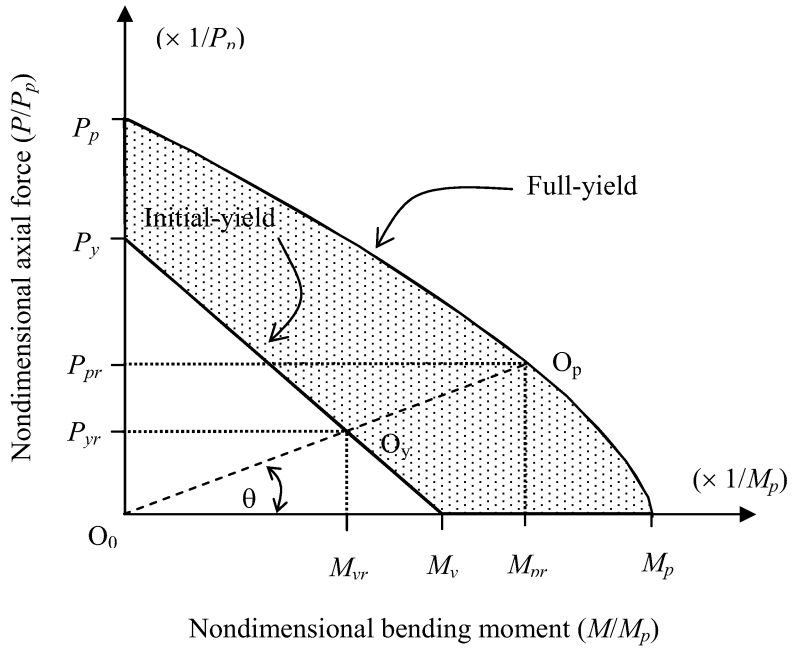

Figure 4. *M*+*P* Initial-yield and Full-yield Capacities

4.2 Moment Plus Shear Effect

Under some combination of applied bending moment M and shear force V, initial yielding of a member section is governed by the normalized initial-yield criterion,

$$\frac{M}{M_y}+\frac{V}{V_y}=1 \tag{23}$$

which is a straight line as shown in Figure 5. The full yielding of the section can be taken as being governed by the normalized full-yield criterion (Heyman and Dutton [27]),

$$\left(\frac{M}{M_p}\right)+C_1\left[1-\sqrt{1-\left(\frac{V}{V_p}\right)^2}\right]=1 \tag{24}$$

which is plotted as the nonlinear full-yield line (for a specified coefficient C_1) shown in Figure 5. The moment and shear force initial-yield and full-yield capacities are M_y, V_y and M_p, V_p, respectively, and in Eq. (24) the coefficient $C_1=A_w/(2A-A_w)$ for a wide-flange section having total area A and web area A_w (e.g., $C_1=0.2$ when $A_w=A/3$). The inelastic response domain for the member section is the shaded area in Figure 5 bounded by Eq. (23) and Eq. (24), and the linear full-yield in shear line $V/V_p=1$.

As shown in Figure 5, the region of influence in the inelastic response domain for a particular combination of moment M plus shear force V is defined by the angle of inclination Θ of the straight line that passes through the origin point O_o and points O_y and O_p corresponding to first-yield and full-yield of the section, respectively. Figure 5 also indicates that point O_y corresponds to reduced first-yield moment and shear force capacities M_{yr} and V_{yr}, respectively, while the point O_p corresponds to reduced full-yield moment and shear force capacities M_{pr} and V_{pr}, respectively. Having, from the analysis, the coordinates (M_{yr}/M_p, V_{yr}/V_p) of the first-yield point O_y for a

particular combination of M plus V causing plastic deformation at an end section of a beam-column member, the angle of inclination of line O_o-O_y-O_p in Figure 5 is readily found as,

$$\Theta = \tan^{-1}\left[\frac{V_{yr}M_p}{M_{yr}V_p}\right] \tag{25}$$

which is used to calculate the initial and full yield capacities of shear forces and bending moments.

Having the reduced first-yield and full-yield moment capacities M_{yr}, and M_{pr} determined, the inelastic flexural stiffness R accounting for the combined bending moment and shear force case can be facilitated by replacing the moment capacities M_y and M_p in Eq. (3) with associated reduced moment capacities M_{yr} and M_{pr}, respectively. Similarly, the transverse shear stiffness T can be obtained by substituting V_y and V_p in Eq. (8) with the reduced first-yield and full-yield capacities V_{yr}, and V_{pr}, respectively. Then, the corresponding stiffness degradation factors r and t can then be computed from Eq. (4) and (8), respectively.

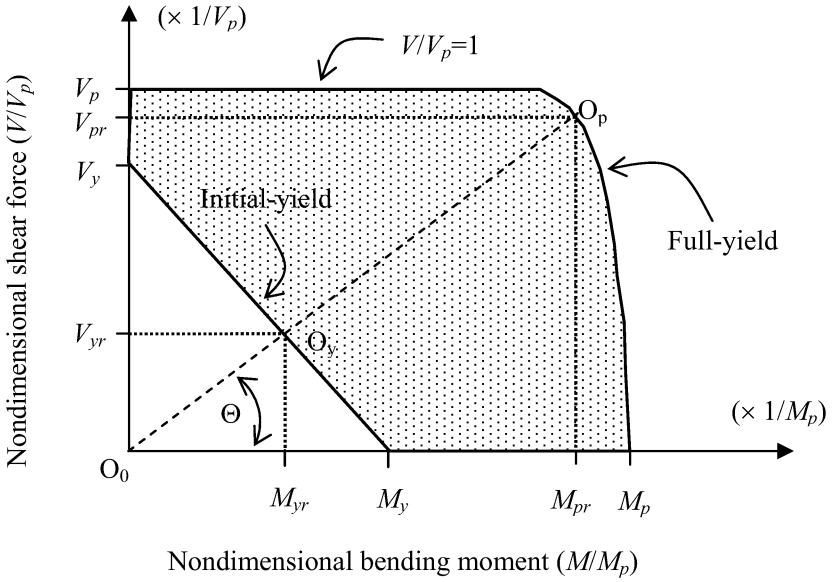

Figure 5. M+V Initial-yield and Full-yield Capacities

5. INCREMENTAL COMPUTATION PROCEDURE

The nonlinear analysis is an incremental-load procedure that, for each load increment, involves formulating and solving the equilibrium equations,

$$\boldsymbol{K}\Delta\boldsymbol{u} = \Delta\boldsymbol{F} \tag{26}$$

where $\boldsymbol{K}$ = structure stiffness matrix, $\Delta\boldsymbol{u}$ = vector of incremental nodal displacements, $\Delta\boldsymbol{F}$ = vector of incremental equivalent joint loads due to external load $\Delta\lambda\boldsymbol{P}$, $\Delta\lambda$ = proportionally applied incremental load factor, and $\boldsymbol{P}$ = total designated external load. In order to facilitate identification of load levels at which plastic deformation of members is initiated, the magnitude of the load-factor increment is decreased over the loading history as (Grierson et al. [28]),

$$\Delta\lambda_1 = \Delta\lambda^*; \quad \Delta\lambda_i = \Delta\lambda_{i-1}(1-\Delta\lambda^*) \quad (i = 2, 3, ...) \tag{27}$$

where $\Delta\lambda^* < 1$ is an initially specified small value selected to ensure initial-order linear-elastic behavior of the structure for the initial load increment. If the structure stiffness matrix $\boldsymbol{K}$ is nonsingular at the end of an incremental load step, Eq. (26) is solved for incremental nodal displacements $\Delta\boldsymbol{u}$. Incremental member-end forces $\Delta\boldsymbol{f}$ and deformations $\Delta\boldsymbol{d}$ are found. Next, total nodal displacements $\boldsymbol{u} = \Sigma\Delta\boldsymbol{u}_i$, member-end forces $\boldsymbol{f} = \Sigma\Delta\boldsymbol{f}_i$ and deformations $\boldsymbol{d} = \Sigma\Delta\boldsymbol{d}_i$ accumulated thus far over the load history are found. The initial-yield and full-yield conditions for each member-end section are checked to detect plastic behavior, and corresponding flexural stiffness degradation factors r are found and applied to modify member stiffness matrices $\boldsymbol{k}$, and hence the structure stiffness matrix $\boldsymbol{K}$, before commencing the next load step. The incremental-load analysis procedure continues until the designated ultimate load $\boldsymbol{P}$ is reached (i.e., final $\lambda_f = \Sigma\Delta\lambda_i = 1$), or a member failure is detected, or the structure stiffness matrix $\boldsymbol{K}$ becomes singular as a consequence of failure of part or all of the structure at a lower load level (i.e., $\lambda_f = \Sigma\Delta\lambda_i < 1$). The analysis results include the values of the inelastic stiffness degradation factors r and t indicating the extent of plastic deformation of members. Further computational details are provided through the analysis examples presented in the following section.

6. EXAMPLES AND ANALYSES

Three examples are presented in this section to illustrate the analytical procedure and verify the correctness of the proposed method. Comparisons are made between the proposed method and to other published methods in each example to show the effectiveness and the accuracy on predicting the inelastic behavior of steel structures accounting for the flexural and shear stiffness degradations.

6.1 Example 1

To verify the proposed method, the portal frame shown in Figure 6(a) is investigated as the first example, which is of particular significance since it was studied by Kanchanalai [19] for the development of the beam-column interaction equations of the AISC-LRFD Specification [2]. Attalla et al. [14] also analyzed the example in their research as a benchmark. All members are of W200×46 section with critical slenderness ratio 40 which yields the length of the column to be $L_c = 3.524$ m. To satisfy the requirement of $G_u = 2$, $L_b = 2L_c$ should be held, where the definition of G_u is shown in Figure 6(a). Based on the results of Attalla et al. (1994), the yield stress F_y is taken as 250 MPa.

Adopting the foregoing properties, the results of the frame obtained from the proposed nonlinear inelastic analysis are shown in Figure 4(b) for the major axis bending case. As previously described, the loading pattern of the frame is such that the gravity load P is applied incrementally from zero to a given target value (say 100 kN), then the horizontal load H is applied incrementally from zero to the load level at which either the plastic collapses or inelastic instability occurs. Given different target values of the gravity load, the corresponding horizontal collapse loads can be obtained from the analysis. Thus, the relationship between vertical and horizontal loads (H and P) at the collapse state is established as the solid curve shown in Figure 6(b). It can be seen from Figure 6(b) that the obtained analysis results are in very good agreement with those obtained by Kanchanalai [19] and Attalla et al. [14].

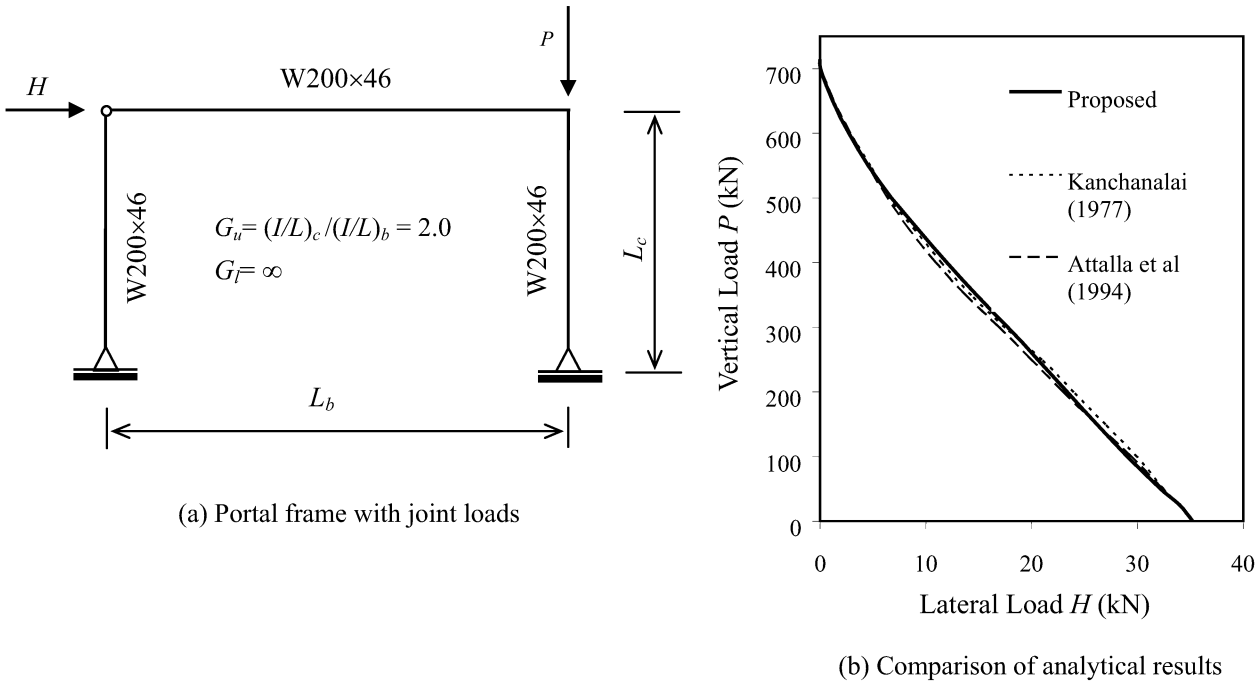

(a) Portal frame with joint loads

(b) Comparison of analytical results

Figure 6. Inelastic Analysis of Portal Frame

6.2 Example 2

The second example presents a two-span continuous beam subjected to the pattern of concentrated point loading shown in Figure 7, for which the experimental results were reported by Driscoll and Beedle [20]. The ultimate total load is taken as W=1000 kN. The steel beam is a wide-flange W12×36 section with the following section properties: section depth d = 312.42 mm (12.30 in), flange width b_f = 168.28 mm (6.625 in), flange thickness t_f = 13.06 mm (0.514 in), web thickness t_w = 8.56 mm (0.337 in), cross section area A = 6954.82 mm^2 (10.78 in^2), moment of inertia I_x = 117.42 × 10^6 mm^4 (282.1 in^4), plastic modulus Z_x = 848.69 × 10^3 mm^3 (51.79 in^3), and shape factor f = 1.13. There is no axial force (P = 0) for the beam in investigation. Plastic deformation may occur at each load point B, C, E and F, and at interval support point D, and the beam is modeled by 6 elements in all. The results obtained from the proposed method are illustrated in Figure 8.

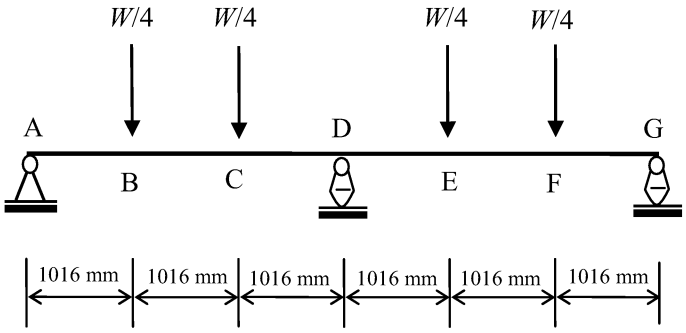

Figure 7. Two-span Beam with Point Loading

The nonlinear incremental-load analysis terminated when the beam failed at load factor level λ_f =

0.996 (i.e., at total load level $\lambda_f \times W = 0.996 \times 1000 = 996$ kN). Over the loading history up to failure, the beam developed two fully-plastic sections at points B, D and F at load-factor levels $\lambda = 0.992$ and 0.996, respectively. Plastic deformation of plastic-hinge section D is associated with both fully degraded flexural stiffness and fully degraded shearing stiffness (i.e., $r = t = 0$). Plastic deformation of plastic-hinges B and F are associated with fully degraded flexural stiffness alone (i.e., $r = 0$ and $t = 1$). The variation in vertical deflection of point F of the beam during the incremental loading process is defined by the solid line in Figure 8. The beam remained stable until 99.6% of the total load W =1000 kN had been applied, at which point δ_F began to increase dramatically without further increase in load. Numerically, this failure event is characterized by the beam stiffness matrix $\boldsymbol{K}$ becoming singular as the stiffness coefficient associated with vertical deflection of point F tends to zero at load-factor level $\lambda_f = 0.996$.

Also shown in Figure 8 are the experimental results found for the same beam by Driscoll and Beedle [20] who also observed that beam deflections associated with transverse shear deformations were of the same order of magnitude as those associated with flexural deformations. They also reported that shear yielding was observed near the centre support D at a load level which was less than that causing flexural yielding. It is observed from Figure 8 that the results obtained by the proposed analysis method which accounts for both flexural and shear stiffness degradations over the loading history are in good agreement with those obtained from the test. The predicted failure load and corresponding vertical deflection δ_F are 996 kN and 12.42 mm, respectively.

Also presented in Figure 8 are the results in which the shear stiffness degradation is neglected. It is clear that neglecting the shear stiffness degradation would result in a higher predicted failure load (1104 kN) and lower deflection (δ_F = 7.65 mm) due to overestimating the stiffness of the beam.

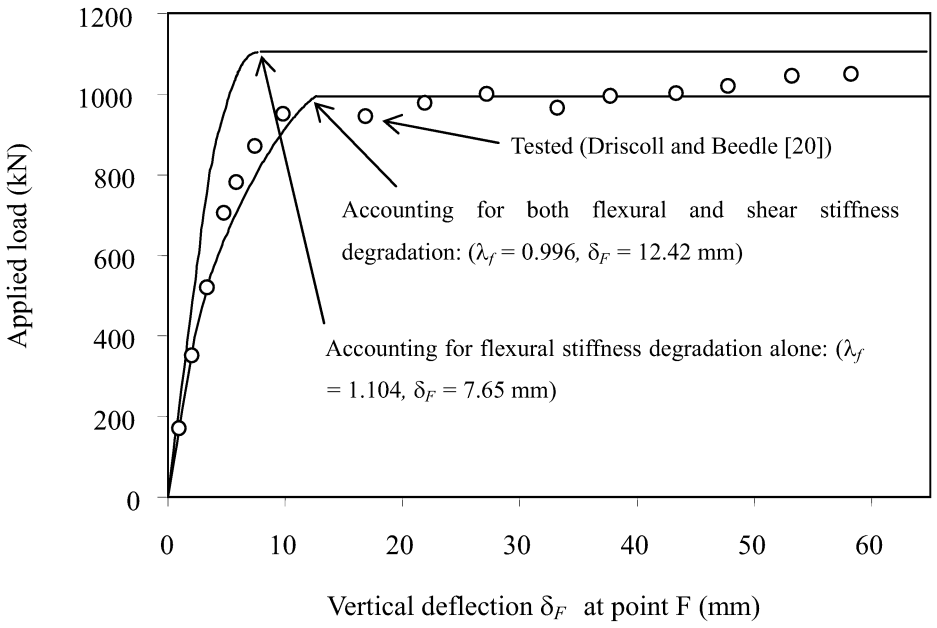

Figure 8. Two-span Beam with Point Loading

6.3 Example 3

The last example is a portal frame subjected to two concentrated vertical loads as shown in Figure 9. This frame was studied with the refined plastic hinge method (Chen et al. [8]). The yield stress of the steel is F_y = 248 MPa. Let both loads increase proportionally with a load factor λ. The collapse load factor λ_c is found to be 1.215 based on rigid-plastic analysis, as shown in Figure 10. By implementing the first-order plastic hinge method without accounting for the effects of P-Δ, and letting $\phi_p = 0$, the analysis yields $\lambda_c = 1.215$ as expected, in which the three plastic hinges form sequentially as shown in Figure 10.

The results from the proposed nonlinear inelastic analysis in a parametric study on plastic limit curvature are shown in Table 1. When taking $\phi_p = 0$, the proposed method is simpler than second-order plastic-hinge analysis. With the increased value of ϕ_p, the collapse load factor λ_c decreases slightly, but the displacement at the collapse state increases considerably. When ϕ_p is taken as 0.0025, the load-deflection curve in Figure 6 approaches that obtained by Chen et al. [8]), and the results obtained by these two methods are in good agreement. It is noted from Table 1 and Figure 6 that with the variation of the value of ϕ_p, the difference of limit or collapse loadings is insignificant, but the differences in the displacements at the corresponding limit states vary considerably. However, by adopting parameter ϕ_p between 0.0015 and 0.0035, the results are in agreement with reported test results (Kusuda and Thurlimann [29]). Therefore, the ϕ_p value within the foregoing range (e.g. 0.0025) is recommended for use in the proposed nonlinear analysis.

7. SUMMARY AND CONCLUSIONS

Presented in this paper is an analysis method for investigating the behavior of steel frameworks accounting for geometric and material nonlinearities. The proposed flexural and shearing stiffness degradation factors provide a simplistic way to account for the inelastic behaviour of beam-column members in the proposed nonlinear analysis method. In addition, the factors also provide valuable information for assessing the strength, stiffness and stability of the individual member and that of the structure as a whole. The three examples demonstrate that the proposed nonlinear analysis method appropriately simulates the inelastic behavior of steel framed structures accounting for the influences of both flexural and shearing inelastic stiffness degradations. The results obtained by the proposed method in the two portal frameworks and one two-span continuous beam are in good agreement with those of other analysis methods and experimental results.

The parametrical study with respect to plastic limit curvature ϕ_p presented in Figure 10 shows that the analysis results associated with ϕ_p ranging between 0.0015 and 0.0035 rad/per unit length are consistent with the experimental results carried out by Kusuda and Thurlimann [29]) and the analytical model proposed by Attalla et al. [14]). For the reason of simplicity, $\phi_p = 0.0025$ rad/per unit length is recommended to be used in practice. The primary advantages of the proposed method are simplicity, practicality and efficiency. Compared to the conventional inelastic analysis, the proposed analysis accounts for shear stiffness degradation which realistically predicts the shear failure associated with abnormal loading events (Grierson et al. [28]). The bending and shearing stiffness degradation factors introduced in this study quantify the formation and intensity of inelasticity of member cross sections and are convenient for structural design.

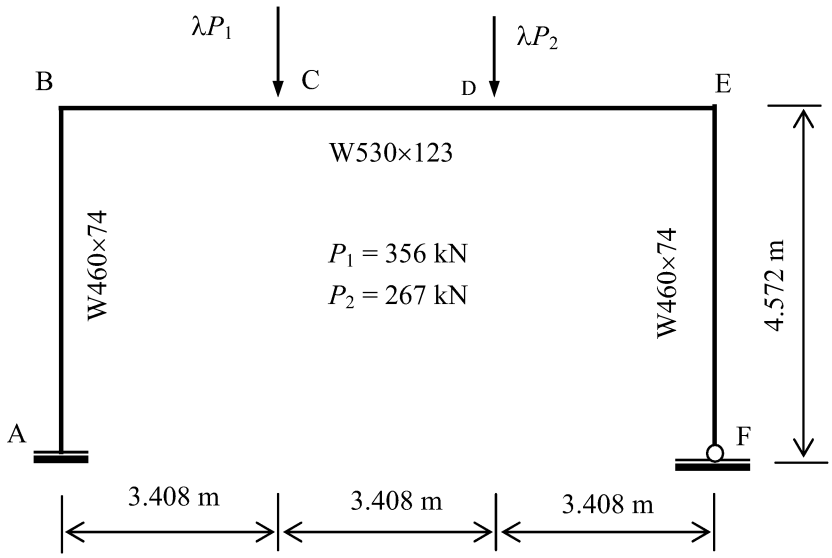

Figure 9. Portal Frame with Vertical Loads

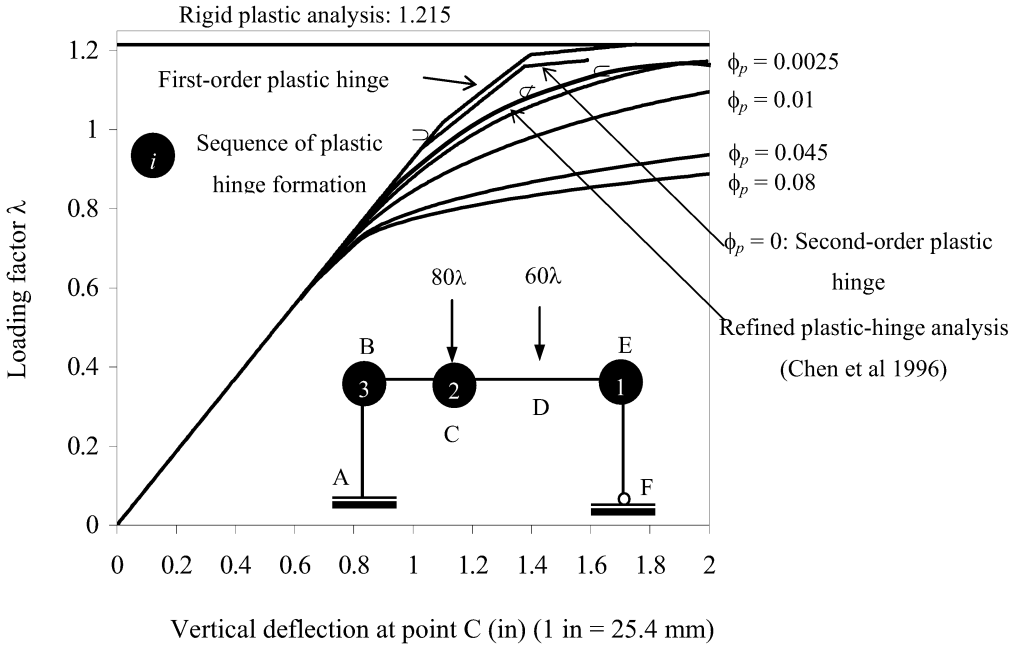

Figure 10. Load vs Deflection with Different Analysis Models

Table 1. Comparison of Collapse Load Factor λ_c

Method	2nd-order plastic hinge	2nd-order refined plastic hinge	Proposed nonlinear inelastic analysis			
			ϕ_p =0.0025	ϕ_p =0.01	ϕ_p =0.045	ϕ_p =0.08
Chen et al.	1.166	1.170	-	-	-	-
Present study	1.176 (ϕ_p=0)	-	1.171	1.171	1.160	1.150

ACKNOWLEDGEMENTS

This work was funded by a research grant (RGPIN203154) from the Natural Science and Engineering Research Council of Canada.

REFERENCES

[1] McGuire, W., Gallagher, R.H. and Ziemian, R.D., "Matrix Structural Analysis", 2nd Edition. John Wiley & Sons, Inc., New York, 2000.
[2] CISC (Canadian Institution of Steel Construction), "Handbook of Steel Construction", 8th Ed., Universal Offset Limited Alliston, Ontario, Canada, 2004.
[3] AISC (American Institute of Steel Construction), "Manual of Steel Construction-Load and Resistance Factor Design (LRFD)", 3rd Edition, Chicago, Illinois, 2001.
[4] CEN, "Eurocode 3: Design of Steel Structures", Part 1.8 – Design of Joints, European Standard, Brussels, Belgium, 2002.
[5] Ziemian, R.D., McGuire, W. and Deierlein, G.G., "Inelastic Limit States Design Part I: Planar Frame Structures", J. Struct. Engrg., ASCE, 1992, 118(9), pp. 2532-2549.
[6] Chen, W.F. and Toma, S., "Advanced Analysis of Steel Frames", CRC Press: Boca Raton, 1994.
[7] Orbison, J.G., McGuire, W. and Abel. J.F., "Yield Surface Application in Nonlinear Steel Frame Analysis", Computer Methods in Applied Mechanics and Engineering, 1982, 33(1-3).
[8] Chen, W.F., Goto, Y. and Liew, J.Y.R., "Stability Design of Semi-rigid Frames", John Wiley & Sons, Inc., New York, 1996.
[9] King, W., White, D.W. and Chen, W.F., "Second-order Inelastic Analysis Methods for Steel-frame Design", J. Struc. Engrg, ASCE, 1992, 118(2), pp. 408-428.
[10] Acroyd, M.H., "Nonlinear Inelastic Stability of Flexible-Connected Plane Steel Frame", Ph.D. Thesis, Department of Civil Engineering, University of Colorado, Boulder, CO, 1979.
[11] Cook, N.E., Jr., "Strength and Stiffness of Type 2 Steel Frames", Ph.D. Thesis, Department of Civil Engineering, University of Colorado, Boulder, CO, 1983.
[12] Espion, B., "Nonlinear Analysis of Framed Structures with a Plasticity Mined Element", Computer and Structures, 1986, 22(5), pp. 831-839.
[13] Powell, G. H. and Chen, P.F.S., "3D Beam-collum Element with Generalized Plastic Hinges", J. Eng. Mech., ASCE, 1984, 112(7), pp. 627-641.
[14] Attalla, M.R., Deierlein, G.G. and McGuire, W., "Spread of Plasticity: Quasi-plastic-hinge Approach", J. Struct. Engrg., ASCE, 1994, 120(8), pp. 2451-2473.
[15] Chan, S.L. and Zhou, Z.H., "Elastoplastic and Large Deflection Analysis of Steel Frames by One Element Per Member, II: Three Hinges Along Member", J. Struct. Engrg., ASCE, 2004, 130(4), pp. 545-553.
[16] Timoshenko, S.P. and Gere, J.M., "Theory of Elastic Stability", McGraw-Hill, New York, 1961.
[17] Chugh, A.K., "Stiffness Matrix for a Beam Element Including Transverse Shear and Axial Force Effects", International Journal for Numerical methods in Engineering, 1977, 11, pp.1681-1697.
[18] Chen, W.F. and Lui, E.M., "Stability Design of Steel Frames", CRC Press, Inc. Florida: Boca Raton, 1991.
[19] Kanchanalai, T., "The Design and Behavior of Beam-columns in Unbraced Steel Frames", CESRL Report No. 77-2, University of Texas, Austin, Tex, 1977.
[20] Driscoll, G.C. and Beedle, L.S., "The Plastic Behavior of Structural Members and Frames", The Welding Journal, 1957, 36(6): pp. 275-s.

[21] Huber, A.W. and Beedle, L.S., "Residual Stress and the Compressive Strength of Steel", Welding Journal, 1954, 33(12), pp. 589-614.
[22] Hasan, R., Xu, L. and Grierson, D.E., "Push-over Analysis for Performance-based Seismic Design", Journal of Computers & Structures, 2002, 80, pp. 2483-2493.
[23] Liu, Y., "Failure Analysis of Building Structures Under Abnormal Loads", Research Report, Dept. of Civil Engineering, University of Waterloo, Ontario, Canada, 2004.
[24] Xu, L. and Grierson, D.E., "Computer-automated Design of Semirigid Steel Frameworks", Journal of Structural Engineering, ASCE, 1993, 119(6), pp. 1740-1760.
[25] Hall, W.J. and Newmark, N.M., "Shear Deflection of Wide-flange Steel Beams in the Plastic Range", ASCE Transactions, 1957, 122, pp. 666-687.
[26] Duan, L. and Chen, W.F., "A Yield Surface Equation for Doubly Symmetrical Sections", Eng. Struct., 1990, 12(2), pp. 114-119.
[27] Heyman, J. and Dutton, V.L., "Plastic Design of Plate Girders with Unstiffened Webs", Welding and Metal Fabrication, 1954, 22, pp. 256.
[28] Grierson, D.E., Xu, L. and Liu, Y., "Progressive-failure Analysis of Buildings Subjected to Abnormal Loading", Journal of Computer-Aided Civil and Infrastructure Engineering, 2005, 20(3), pp. 155-171.
[29] Kusuda, T. and Thurlimann, B., "Strength of Wide Flange Beams under Combined Influence of Moment, Shear and Axial Force", Frits Engineering Laboratory Report No. 248.1. Lehigh University, 1958.